Communications in Theoretical Physics

Commun. Theor. Phys. **76** (2024) 125402 (14pp) https://doi.org/10.1088/1572-9494/ad745f

Traversable wormhole solutions utilizing the Karmarkar condition in $f(\mathcal{R},\mathcal{G})$ gravity

Tayyaba Naz[1], Adnan Malik[2,3,*], M Z Bhatti[4], M Kamran Asif[1] and Iffat Fayyaz[1]

[1] National University of Computer and Emerging Sciences, Lahore Campus, Pakistan
[2] School of Mathematical Sciences, Zhejiang Normal University, Jinhua, Zhejiang, China
[3] Department of Mathematics, University of Management and Technology, Sialkot Campus, Lahore, Pakistan
[4] Department of Mathematics, University of the Punjab, Quaid-i-Azam Campus, Lahore-54590, Pakistan

E-mail: tayyaba.naz@nu.edu.pk, adnanmalik_chheena@yahoo.com, adnan.malik@skt.umt.edu.pk, mzaeem.math@pu.edu.pk, kamranmurtaza38@gmail.com and iffat845@gmail.com

Received 21 April 2024, revised 14 August 2024
Accepted for publication 21 August 2024
Published 22 October 2024

Abstract

The main objective of this paper is to reveal the evolving traversable wormhole solutions in the context of modified $f(\mathcal{R}, \mathcal{G})$ gravity, which affects the gravitational interaction. These results are derived by applying the Karmarkar condition, which creates wormhole geometry that meets the necessary conditions and connects two asymptotically flat areas of spacetime. The proposed study's main goal is to construct the wormhole structures by splitting the $f(\mathcal{R}, \mathcal{G})$ gravity model into two forms Firstly, we split the model into an exponential-like $f(\mathcal{R})$ gravity model and a power law $f(\mathcal{G})$ gravity model, and secondly, we consider the Starobinsky $f(\mathcal{R})$ gravity model along with a power law $f(\mathcal{G})$ gravity model. Besides, we address the feasibility of shape functions and the structural analysis of wormhole structures for specific models. These models are then confined to be compatible with current experimental evidence. Further, the energy conditions of the wormhole are geometrically probed, and it is proven that they adhere to the null energy conditions in areas close to the throat. Moreover, the fascinating aspect of this study involves conducting an examination and comparison of evolving wormhole geometries in the vicinity of the throat in our chosen models, utilizing two- and three-dimensional graphical representations. We observe that our shape function acquired through the Karmarkar technique yields validated wormhole configurations with even less exotic matter, correlating to the proper choice of $f(\mathcal{R}, \mathcal{G})$ gravity models and acceptable free parameter values. In summary, we conclude that our findings meet all the criteria for the existence of wormholes, affirming the viability and consistency of our study.

Keywords: Wormhole Structures, $f(\mathcal{R}, \mathcal{G})$ gravity, karmarkar condition, shape function

(Some figures may appear in colour only in the online journal)

1. Introduction

The pursuit of understanding the fundamental nature of the Universe has led researchers to explore the enigmatic realm of wormholes (WHs). The investigation of WH solutions is an intriguing subject of discourse in cosmological literature. These are essentially tunnel geometries that link various parts of spacetime or completely separate spacetimes. Theoretical tunnels in spacetime, postulated to link far-flung cosmic areas, present an intriguing pathway for exploring the intricacies of gravity and its influence on the spacetime continuum. WHs are often divided into static and dynamic categories. In general relativity (GR), the formation of static WHs necessitates the use of exotic matter (EM)—a hypothetical form of matter with negative energy density, which violates the null energy condition (NEC). One of the pivotal

* Author to whom any correspondence should be addressed.

aspects of WH research revolves around the concept of traversability. While theoretical models suggest the existence of WHs, their practical utility for interstellar travel hinges on the presence of EM. The exploration of how different gravitational environments may influence the creation and sustenance of EM within WHs is a critical aspect of our investigation. The concept of WH hypothetical tunnels in spacetime that could connect distant points in the Universe, has captivated the imagination of physicists and astrophysicists for decades. The seminal work of Albert Einstein and Nathan Rosen [1] paved the way for the conceptualization of these cosmic shortcuts, igniting a journey into the depths of theoretical physics. These cosmic shortcuts, also known as Einstein–Rosen bridges, are theorized to be bridges between separate points in spacetime, potentially allowing for faster-than-light travel. Einstein and Rosen were the ones who initially proposed the idea of a spacetime bridge or tunnel and investigated the exact results that describe the bridge's geometrical design. The answer proposed by Einstein and Rosen is related to Flamm's work [2]. He established the isometric embedding of the Schwarzschild solution for the first time. A drainhole is another name for a WH. The throat radius of a static WH setup is fixed, but the throat radius of a non-static WH design is flexible. Kar [3] investigated the characteristics of static WHs and presented examples. Initially, Morris and Thorne [4] proposed the concept of traveling through WH tunnels. They provided the theory for traversable WHs and used the concepts of GR to analyze static spherically symmetric WHs. In the presence of EM, WHs are the classical answer to Einstein's gravitational field equations, a kind of matter with negative energy. EM plays an essential role in creating WH structures within the framework of GR. In the presence of EM, the stress-energy tensor violates the NEC. Numerous astrophysicists have sought to investigate the stability of WHs and discovered strategies to prevent or reduce NEC violations.

The phenomenon of self-gravitation and its consequences has a great impact in the field of novel astrophysical research and cosmological background. In the result of this gravitational collapse, some new stellar remnants known as compact stars are produced. These compact stars are considered to be very dense as they possess large masses but volumetrically small radii. In relativistic astrophysics, compact stars have drawn the attention of the researcher due to their captivating characteristics and relativistic structures. Our universe often exhibits eye-opening challenges for cosmologists, regrading their fascinating and enigmatic existence. The theory of GR has been modified in various ways in the literature [5–9]. One such modification, the $f(\mathcal{R})$ gravity theory [10], has been adopted by numerous researchers to describe the expanding Universe. This theory replaces the scalar curvature $\mathcal{R}$ with an arbitrary function $f(\mathcal{R})$ in the gravitational action. Starobinsky [11] studied the $f(\mathcal{R})$ model with $f(\mathcal{R}) = \mathcal{R} + \alpha\mathcal{R}^2$, where $\alpha > 0$ and found it to represent the inflationary epoch of the early Universe. Furthermore, the scenario to unify inflation with dark energy in a consistent way was proposed in [12]. Moreover, the cosmological models in the context of modified theories are explored in [13–23].

Recent observations indicated a rapid expansion of the cosmos [24–26]. In this regard researchers recently examined the geometry of WH in several modified theories of gravity (MTG) [27–33]. The MTG are very useful for describing the cosmic expansion and other related ideas. Sharif and Zahra [34] investigated static traversable WH solutions within the framework of $f(\mathcal{R})$ gravity, they demonstrated that WH solutions are feasible when considering barotropic matter. Additionally, Mishra *et al* [35] discussed traversable WH solutions under the framework of $f(\mathcal{R}, \mathcal{T})$ gravity. Hence, exploring traversable WH solutions with various modifications in the context of MTG could be intriguing for further research. Shamir and Zia [36] investigated the existence of static traversable WH near the throat within the framework of $f(\mathcal{R}, \mathcal{G})$ gravity. In MTG, thin-shell WH existence is permitted when there is higher-order curvature phrases [37]. The cosmic development of WH solutions was discussed in [38]. Sahoo and his colleagues [39, 40] investigated WH solutions in several MTG. Moreover, traversable WH solutions and quantum equations like the Schrödinger and Dirac equations serve different purposes within their respective fields. The study of WHs provides insights into gravitational theories and spacetime structures, while quantum equations and their solutions reveal details about particle behavior and quantum phenomena [41–43]. Each area of research is valuable and complements the broader understanding of physical laws and the Universe. Some other useful work related to WH solutions in the context of MTG can be seen in [44–47]. Bahamonde *et al* [48] investigated WHs using Noether symmetries.

The exploration of WHs in different gravitational environments not only contributes to the theoretical understanding of these exotic phenomena but also holds implications for the potential practicality of utilizing them for interstellar travel. As we unravel the mysteries of WHs amidst varying gravitational influences, we move one step closer to deciphering the secrets of the cosmos and unlocking the doors to new frontiers in spacetime exploration. The analysis of the WH shape function (WSF) and its core attributes is a captivating facet within the realm of traversable WH geometry. To characterize the WH structure, numerous authors have studied the ansatz shape function. In order to delineate the structure of a WH, several researchers have explored the ansatz shape functions. An asymptotically flat WH examined by Godani and Samanta [49] using the WSF i.e. $\epsilon(r) = \frac{r_0 \mathrm{Log}(r+1)}{\mathrm{Log}(r_0+1)}$. Cataldo and Liempi [50] employed the WSF $[\epsilon(r) = \alpha + \beta(r)]$ to investigate the geometry of WH. Jahromi and Moradpour [51] introduced a WSF in the form of $\epsilon(r) = a \tanh r$. Samanta *et al* [52] formulated a shape function in the form $\epsilon(r) = \frac{r}{e^{r-r_0}}$, referred to as the exponential WSF, to explore solutions of WH.

For stable physical models, one method involves using an analytical approach with Einstein's Field Equations (EFE) and considering a four-dimensional manifold that can be mapped into Euclidean space. By embedding curved geometries into higher-dimensional spaces, one can derive various exact solutions for astrophysical stellar systems. Nash [53] subsequently introduced the isometric embedding

theorem. The embedding class-one approach has been utilized to study several aspects of anisotropic compact objects, as detailed in the literature [54–61]. Gupta and Gupta [62] examined non-static fluid distributions with non-vanishing acceleration, while Gupta and Sharma [63] explored embedding class-I solutions for non-static perfect fluids using a plane-symmetric metric. The embedding class constraint results in a differential equation, known as the Karmarkar condition, which relates two components of metric potentials in static spherically symmetric geometries. Karmarkar [64] was the first who illustrated the compulsory condition for a static spherically symmetric spacetime to be of embedding 1, which is very helpful to find the exact solutions of field equations. This allows for a more detailed and exact analysis of the interior structure of relativistic stars, facilitating the study of their geometric properties under the influence of anisotropic pressure distributions. The Karmarkar condition, expressed as $R_{1414}R_{2323} = R_{1212}R_{3434} + R_{1224}R_{1334}$, connects the metric tensor components g_{rr} and g_{tt} for a spherically symmetric fluid distribution. Extensive work has been done on this condition [65–67], linking these metric components. Maurya *et al* [68] and Bhar *et al* [69] applied the Karmarkar condition to the EFE, finding stable solutions that are useful for studying stellar interiors. More recently, Sharif and Saba [70] investigated charged anisotropic solutions within the $f(\mathcal{G})$ gravity framework, identifying physically consistent and stable solutions. Additionally, Upreti *et al* [71] have presented a new set of embedded solutions using the Karmarkar condition.

No astrophysical object in the real universe is composed entirely of perfect fluid, where principal stresses are equal. The central energy density of such compact objects can reach approximately 10^{15} g cm^{-3}, several times higher than the normal nuclear matter density. Theoretical investigations [72–77] on realistic stellar models strongly suggest that the matter distribution in these massive stellar objects may be locally anisotropic, meaning the radial pressure may not equal the tangential pressure, particularly in very high-density ranges. The analytic solution by Bowers and Liang [78] of anisotropic spheres with uniform energy density demonstrated that anisotropy can also play a significant role in describing high-redshift objects like quasars. Anisotropy in pressure can significantly affect physical parameters such as the maximum compactness, mass and radius of a star. Initially, cosmologists believed that the inner structure of compact objects was described only by perfect fluid. While isotropy may have certain suitable attributes, it does not reflect the typical characteristics of compact stars. In cosmology, anisotropic fluid has gained significant attention as an alternative to isotropic matter distribution. Anisotropic matter is used to describe the phase development and internal characterization of stellar configurations. Anisotropy in the fluid can arise from the amalgamation of different categories of fluids, magnetic fields, viscosity, rotation, etc. Anisotropy in stellar structures can result from phase transitions, stars with pion condensation [79], electromagnetic fields [80–82], the presence of a solid core, and other factors. Anisotropy is a more realistic representation of stellar interiors, especially in highly dense objects where different types of stresses and pressures do not necessarily align. The Karmarkar condition, when coupled with anisotropic fluid distributions, can yield more accurate models of these celestial bodies, providing insights into their stability and evolution. Conducting detailed numerical simulations of anisotropic stars and wormholes using the Karmarkar condition can help in validating theoretical predictions and improving the accuracy of models.

The goal of this paper is to investigate various possible regions for the presence of WH solutions in $f(\mathcal{R}, \mathcal{G})$ gravity. Firstly we develop the WSF by using the Karmarkar technique. Karmarkar [64] developed a mandatory condition for a static and spherically symmetric line element to be of class-one. In recent years, different researchers have considered the Karmarkar condition to discuss the configurations of spherically symmetric compact objects [83–86]. Maurya *et al* [87] investigated an anisotropic compact star in the GR context using an embedding class-one methodology. They assessed many aspects of compact stars in the presence of an anisotropic fluid distribution and concluded that the results accurately portrayed the interior of stellar formations. It is also to note that Salako *et al* [88] have studied the existence of strange starts in $f(\mathcal{T}, \mathcal{T})$ gravity, where $\mathcal{T}$ be the torsion tensor. Naz *et al* [89] have used the Karmarkar condition to find the physically acceptable solution for compact star in $f(\mathcal{R}$ gravity. In $f(\mathcal{R}, \mathcal{T})$ gravity, Ahmed and Abbas [90] studied the gravitational collapse using the Karmarkar condition to the spherically symmetric non-static radiating star. Furthermore, Kuhfittig [91] developed WH geometry using the Karmarkar condition and show that the embedding theory may provide the basis for a complete WH solution.

Next, to discuss the geometry of WHs we partitioned the $f(\mathcal{R}, \mathcal{G})$ gravity model into two ways: firstly, we split the model into an exponential like $f(\mathcal{R})$ model and a power law $f(\mathcal{G})$ gravity model and secondly we consider the Starobinsky $f(\mathcal{R})$ gravity model along with $f(\mathcal{G})$ gravity power law model. Further, EC of the WH are geometrically probed and it is proven that they adhere to the NEC in areas close to the throat. Our present work plan is as follows. In section 2, the discussion revolves around the WH metric and the prerequisites that the shape function must adhere to. Some basic formalism of the $f(\mathcal{R}, \mathcal{G})$ theory of gravity has been investigated in section 3. In the same section, we considered two compatible models of $f(\mathcal{R}, \mathcal{G})$ gravity and discussed the EC*s* with graphical analysis. Additionally, we conduct a comparative analysis of the developing WH geometries near the throat of our considered models, employing two and three-dimensional visual representations. The comparison of our current research work with past related work has been discussed in section 4. Lastly, we have concluded our work in section 5.

2. Construction of wormhole shape function

In this study, our objective is to construct the WSF using the Karmarkar condition. To achieve this, we focus on the static

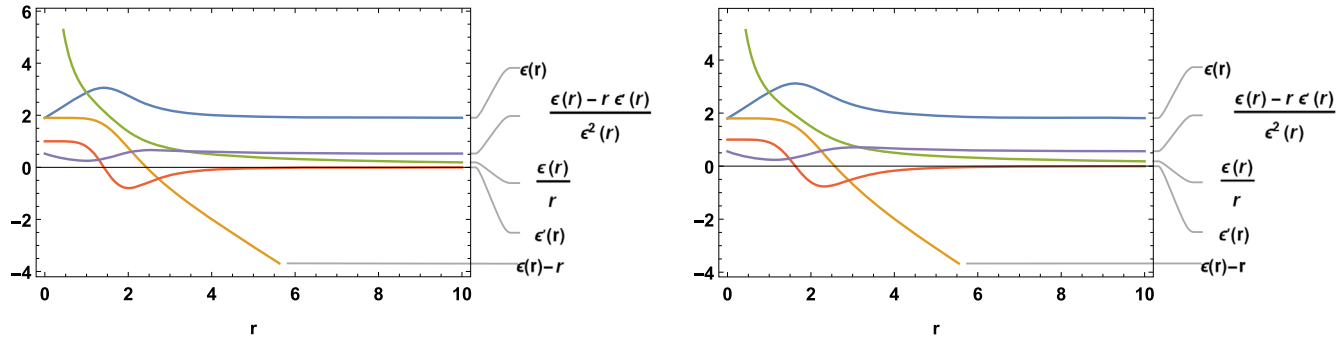

Figure 1. Analysis of WSF for $c = 1.9$ (1st Plot) and $c = 1.8$ (2nd Plot).

spherically symmetric spacetime [92], described as:

$$ds^2 = e^{\chi}dt^2 - e^{\psi}dr^2 - r^2(d\theta^2 + \sin^2\theta d\phi^2). \tag{1}$$

Here, both χ and ψ are functions solely dependent on the radial coordinate. The Riemann curvature values associated with the spacetime (1) are:

$$\mathcal{R}_{1212} = \frac{-e^{\chi}(2\chi'' + \chi'^2 - \chi'\psi')}{4},\ \mathcal{R}_{2323} = \frac{-r\psi'}{2},$$
$$\mathcal{R}_{1414} = \mathcal{R}_{1313}\sin^2\theta,\ \mathcal{R}_{3434} = \frac{r^2\sin^2\theta(e^{\psi-1})}{e^{\psi}},$$
$$\mathcal{R}_{1313} = \frac{-e^{\chi}(r\chi')}{2e^{\psi}},\ \mathcal{R}_{1224} = 0.$$

The non-zero elements mentioned above satisfy the Karmarkar condition.

$$\mathcal{R}_{1414}\mathcal{R}_{2323} = \mathcal{R}_{1212}\mathcal{R}_{3434} + \mathcal{R}_{1224}\mathcal{R}_{1334}, \tag{2}$$

where $\mathcal{R}_{2323} \neq 0$.

By substituting the aforementioned non-zero elements into equation (2), we derive a differential equation in the subsequent form:

$$\frac{\chi'\psi'}{1 - e^{\psi}} = \chi'\psi' - 2\chi'' - \chi'^2,$$

where $e^{\psi} \neq 1$. The solution to the aforementioned differential equation is presented as:

$$e^{\psi} = 1 + Ae^{\chi}\chi'^2. \tag{3}$$

In the above equation, A represents the constant of integration. Moreover, we adopt the Morris–Thorne spacetime to formulate the WSF, defined as:

$$ds^2 = e^{\chi}dt^2 - \frac{1}{1 - \frac{\epsilon(r)}{r}}dr^2 - r^2(d\theta^2 + \sin^2\theta d\phi^2). \tag{4}$$

The parameter χ in the aforementioned metric is the redshift function and is defined as:

$$\chi = \frac{-2\xi}{r}, \tag{5}$$

such that $\chi \to 0$ as $r \to \infty$ and ξ represents the free parameter.

By settings equations (1) and (4), we obtain:

$$\psi = \log\left[\frac{r}{r - \epsilon(r)}\right]. \tag{6}$$

In this context, $\epsilon(r)$ represents a WSF. Utilizing equations (3), (5), and (6), we derive the following expression for the WSF:

$$\epsilon(r) = r - \frac{r^5}{r^4 + 4\xi^2 Ae^{\frac{-2\xi}{r}}}. \tag{7}$$

In order to achieve a traversable WH solution, the shape function must adhere to the conditions delineated by Morris and Thorne [4], specified as:

1. $\epsilon(r)$-$r = 0$ at $r = r_0$,
2. The condition $\frac{\epsilon(r) - r\epsilon'(r)}{\epsilon^2(r)} > 0$ must be filled at $r = r_0$,
3. $\epsilon'(r) < 1$,
4. $\frac{\epsilon(r)}{r} \to 0$ *at* $r \to \infty$.

Here, r denotes the radial coordinate, and r_0 represents the throat radius of the WH, satisfying the condition $r_0 \leqslant r \leqslant \infty$. By evaluating equation (7) at the throat, i.e., $\epsilon(r_0) - r_0 = 0$, a trivial solution is obtained at $r_0 = 0$. To tackle this concern, we introduce a stochastic variable denoted as 'C' into the equation. Now, equation (7) takes the form: $\epsilon(r) = r - \frac{r^5}{r^4 + 4\xi^2 Ae^{\frac{-2\xi}{r}}} + C$. Condition (1) gives, $A = \frac{r_0^4(r_0 - C)}{4\xi^2 e^{\frac{-2\xi^2}{r_0}}}$. Upon substituting the value of A into equation (7), the expression for the WSF $\epsilon(r)$ is obtained as:

$$\epsilon(r) = r - \frac{r^5}{r^4 + r_0^4(r_0 - C)} + C,$$
$$0 < C < r_0. \tag{8}$$

For the value of C in the given range conditions (2) and (3) are fulfilled. Equation (8) takes the form after applying condition (4).

$$\lim_{r\to\infty}\frac{\epsilon(r)}{r} = 0. \tag{9}$$

Asymptotically flat traversable WH are provided by the equation (8). The graphical representation of WSF is shown in figures 1 and 2, which clearly depict that all the conditions are satisfied.

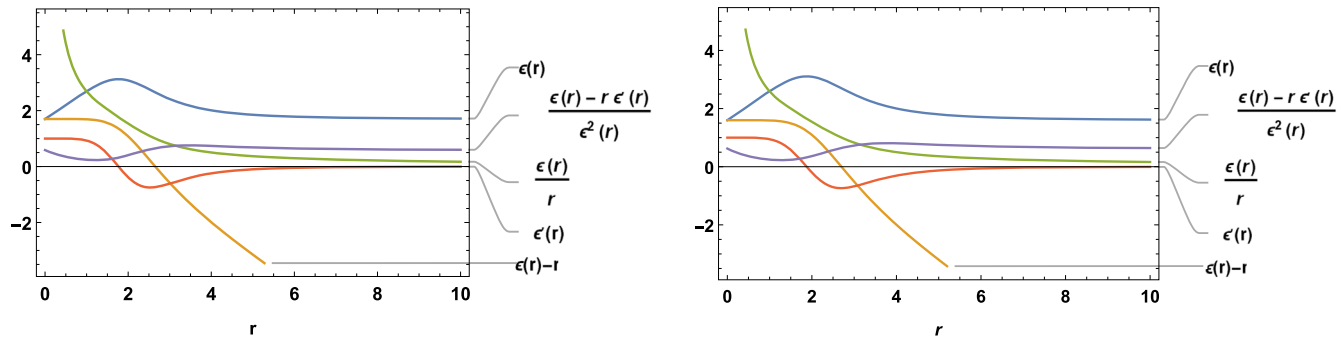

Figure 2. Evaluation of WSF for $c = 1.7$ (1st Plot) and $c = 1.6$ (2nd Plot).

3. Basic formulation and field equations of $f(\mathcal{R}, \mathcal{G})$ theory of gravity

A notable transformation in the theory is achieved by amalgamating the Gauss–Bonnet invariant and scalar curvature terms, giving rise to the paradigm known as $f(\mathcal{R}, \mathcal{G})$ gravity. The application of this theory to observational data has demonstrated its stability and reliability.

The modified Gauss–Bonnet gravity action [93], is expressed as:

$$S = \frac{1}{2\kappa}\int \mathrm{d}^4x\sqrt{-g}f(\mathcal{R}, \mathcal{G}) + \mathcal{S}_{\mathrm{m}}(g_{\zeta\eta}, \psi), \tag{10}$$

where κ stands for the coupling constant and S_{m} represents the matter action. The term associated with the Gauss–Bonnet invariant is expressed as:

$$\mathcal{G} = \mathcal{R}^2 - 4\mathcal{R}_{\zeta\eta}\mathcal{R}^{\zeta\eta} + 4\mathcal{R}_{\zeta\theta\phi\eta}\mathcal{R}^{\zeta\theta\phi\eta}. \tag{11}$$

The modified field equations arise from the variation of the action (10) in terms of the metric tensor.

$$\begin{aligned}
&\mathcal{R}_{\zeta\eta} - \frac{1}{2}g_{\zeta\eta}\mathcal{R} = \kappa T_{\zeta\eta} + \nabla_\zeta\nabla_\eta f_{\mathcal{R}} - g_{\zeta\eta}\,\Box f_{\mathcal{R}}\\
&+2\mathcal{R}\nabla_\zeta\nabla_\eta f_{\mathcal{G}} - 2g_{\zeta\eta}\mathcal{R}\,\Box f_{\mathcal{G}} - 4\mathcal{R}^{\alpha}_{\zeta}\nabla_\alpha\nabla_\eta f_{\mathcal{G}}\\
&-4\mathcal{R}^{\alpha}_{\eta}\nabla_\alpha\nabla_\eta f_{\mathcal{G}} + 4\mathcal{R}_{\zeta\eta}\,\Box f_{\mathcal{G}} 4g_{\zeta\eta}\mathcal{R}^{\alpha\beta}\nabla_\alpha\nabla_\beta f_{\mathcal{G}}\\
&+4\mathcal{R}_{\zeta\alpha\beta\eta}\nabla^\alpha\nabla^\beta f_{\mathcal{G}} - \frac{1}{2}g_{\zeta\eta}V + (1 - f_{\mathcal{R}})\mathcal{G}_{\zeta\eta}.
\end{aligned} \tag{12}$$

In the above equation, the box symbol ($\Box$) represents the Laplacian operator in four dimensions, and the term V is expressed as:

$$V = f_{\mathcal{R}}\mathcal{R} - f(\mathcal{R}, \mathcal{G}) + f_{\mathcal{G}}\mathcal{G}, \tag{13}$$

where, $f_{\mathcal{R}} = \frac{\mathrm{d}f}{\mathrm{d}\mathcal{R}}$ and $f_{\mathcal{G}} = \frac{\mathrm{d}f}{\mathrm{d}\mathcal{G}}$ representing the partial derivatives concerning $\mathcal{R}$ and $\mathcal{G}$, correspondingly. The expression $\mathcal{R}$ appears to be

$$\mathcal{R} = \frac{(2r^2\chi'' + r^2\chi'^2 - r^2\chi'\psi' + 4\chi'r - 4\psi'r - 4e^{\psi} + 4)}{2r^2\mathrm{e}^{\psi}}. \tag{14}$$

In the case of an anisotropic fluid, the energy momentum tensor [94, 95] is given by

$$T_{\alpha\beta} = (\rho + p_{\mathrm{t}})u_\alpha u_\beta - p_{\mathrm{t}}g_{\alpha\beta} + (p_{\mathrm{r}} - p_{\mathrm{t}})\nu_\alpha\nu_\beta, \tag{15}$$

where $\mu_\alpha = \mathrm{e}^{\frac{\chi}{2}}\delta^0_\alpha$, $\nu_\alpha = \mathrm{e}^{\frac{\psi}{2}}\delta^1_\alpha$, The symbol ρ represents density, p_{r} denotes radial pressure and p_{t} represents tangential pressure. $\mathcal{G}$ has the following expression:

$$\mathcal{G} = \frac{2\mathrm{e}^{-2\psi}}{r^2}[(1 - \mathrm{e}^{\psi})(\chi'^2 + 2\chi'' - \chi'\psi') - 2\chi'\psi']. \tag{16}$$

Now, utilizing equations (4)–(12), the field equations are expressed as:

$$\begin{aligned}
\rho = &-\mathrm{e}^{-\psi}f''_{\mathcal{R}} + \left(\frac{-4\mathrm{e}^{-2\psi} + 4\mathrm{e}^{-\psi}}{r^2}\right)f''_{\mathcal{G}}\\
&+\left(\frac{6\mathrm{e}^{-2\psi}\psi' - 2\mathrm{e}^{-\psi}\psi'}{r^2}\right)f'_{\mathcal{G}}\\
&+\mathrm{e}^{-\psi}\left(\frac{\mathrm{r}\chi'(4 + \mathrm{r}\chi' - \mathrm{r}\psi') + 2\mathrm{r}^2\chi''}{4r^2}\right)f_{\mathcal{R}}\\
&+\mathrm{e}^{-\psi}\left(\frac{\mathrm{r}\psi' - 4}{2r}\right)\mathrm{f}'_{\mathcal{R}} + \frac{\mathrm{e}^{-2\psi}}{r^2}\\
&\times[(1 - \mathrm{e}^{\psi})(\chi'^2 - \chi'\psi' + 2\chi'') - 2\chi'\psi']f_{\mathcal{G}} - \frac{f}{2},
\end{aligned} \tag{17}$$

$$\begin{aligned}
p_{\mathrm{r}} = &\frac{2\mathrm{e}^{-2\psi}}{r^2}(-3\chi' + \mathrm{e}^{\psi}\chi')f'_{\mathcal{G}} + \frac{\mathrm{e}^{-\chi}}{2r}(4 + r\psi')f'_{\mathcal{R}}\\
&+\frac{\mathrm{e}^{-\psi}}{4r}(-r\psi'^2 + 4\chi' + r\chi'\psi' - 2r\chi'')f_{\mathcal{R}} - \frac{\mathrm{e}^{-2\psi}}{r^2}\\
&\times[(1 - \mathrm{e}^{\psi})(\chi'^2 - \chi'\psi' + 2\chi'') - 2\chi'\psi']f_{\mathcal{G}} - \frac{f}{2},
\end{aligned} \tag{18}$$

$$\begin{aligned}
p_{\mathrm{t}} = &\frac{\mathrm{e}^{-2\psi}}{r}(2\chi')f''_{\mathcal{G}}\\
&+\mathrm{e}^{-\psi}\mathrm{f}''_{\mathcal{R}} + \frac{\mathrm{e}^{-2\psi}}{r}(\chi'^2 - 3\chi'\psi' + 2\chi'')f'_{\mathcal{G}}\\
&+\frac{\mathrm{e}^{-2\psi}}{2r^2}(2\mathrm{e}^{\psi r} + \mathrm{e}^{\psi r^2}(\chi' - \psi'))f'_{\mathcal{R}} + \frac{\mathrm{e}^{-2\psi}}{2r^2}(2\mathrm{e}^{2\psi}\\
&+\mathrm{e}^{\psi}(-2 - r\chi' + \mathrm{r}\psi'))f_{\mathcal{R}} - \frac{\mathrm{e}^{-2\psi}}{r^2}\\
&\times[(1 - \mathrm{e}^{\psi})(\chi'^2 + 2\chi'' - \chi'\psi') - 2\chi'\psi']f_{\mathcal{G}} - \frac{f}{2}.
\end{aligned} \tag{19}$$

Here, the prime symbol indicates the derivative with respect to the radial coordinate. The expressions for ρ, p_{r}, and p_{t} involve the shape function and the function $f(\mathcal{R}, \mathcal{G})$ along with its radial derivatives. It is worth noting that equations (17)–(19) are highly complex and nonlinear. Consequently, identifying explicit representations for ρ, p_{r}, and p_{t}

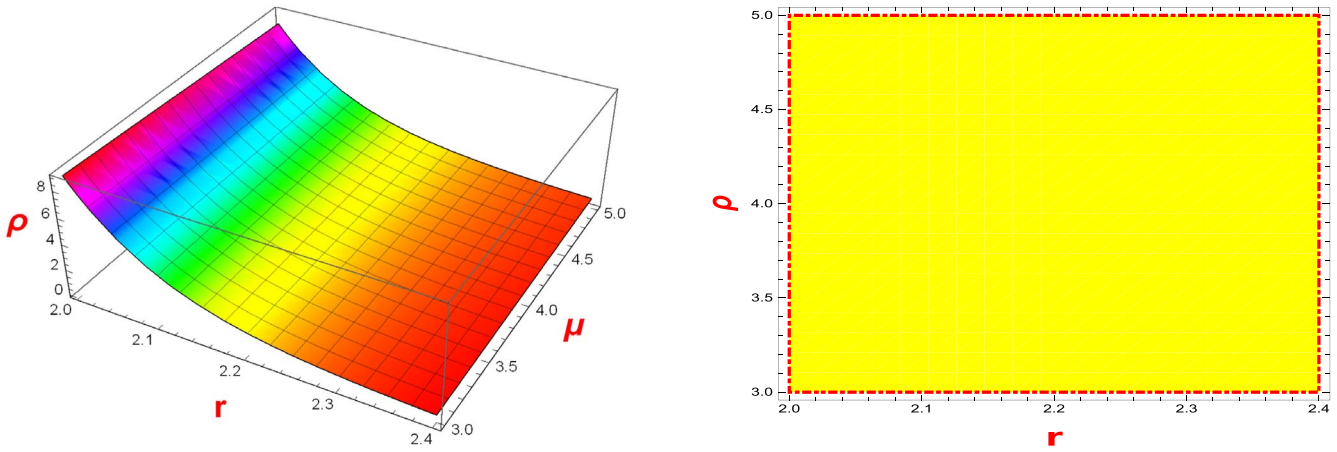

Figure 3. Energy density ρ graphs in 3D and region form.

is challenging. We take a certain kind of function in order to simplify things. The $f(\mathcal{R}, \mathcal{G})$ model is given in below equation:

$$f(\mathcal{R}, \mathcal{G}) = f_1(\mathcal{R}) + f_2(\mathcal{G}). \tag{20}$$

Several feasible models of $f(\mathcal{R}, \mathcal{G})$ theory may be examined by taking into account various forms of $f_1(\mathcal{R})$ and $f_2(\mathcal{G})$. The next subsections examine some well known $f(\mathcal{R}, \mathcal{G})$ models that correlate to $f_1(\mathcal{R})$.

1. $f_1(\mathcal{R}) =$ Exponential gravity model.
2. $f_2(\mathcal{R}) =$ Starobinsky gravity model.

Furthermore, to compute the field equations we take into consideration of power law $f(\mathcal{G})$ gravity model i.e. $f_2(\mathcal{G}) = \gamma\mathcal{G}^2$, γ being an arbitrary constant. One can choose other $f(\mathcal{G})$ gravity models to solve the field equations. The $f(\mathcal{G})$ model remain same with both $f_1(\mathcal{R})$ and $f_2(\mathcal{R})$.

3.1. Model 1: exponential gravity model

Firstly, we consider $f(\mathcal{R}, \mathcal{G}) = f_1(\mathcal{R}) + f(\mathcal{G})$, where $f_1(\mathcal{R})$ is the exponential gravity model and $f(\mathcal{G})$ is the power law model to discuss the traversable WH solutions in frame of $f(\mathcal{R}, \mathcal{G})$ gravity. The exponential gravity model is presented and examined by Cognola *et al* [96]. This model accurately and naturally depicts the acceleration of the Universe current expansion and the inflation of the early cosmos, expressed as:

$$f_1(\mathcal{R}) = \mathcal{R} + \mu\,\nu[e^{\frac{-\mathcal{R}}{\nu}} - 1]. \tag{21}$$

Here, μ and ν represent free variables. A class of exponential, realistic modified gravities was presented by Cognola *et al* [96] in which they argued that this model (20) passes all the local tests including non-violation of Newton's law and stability of spherical body solution. Nojiri and Odintsov [6] investigated this model (14) to describe the early-time inflation and late-time cosmic acceleration in a natural, unified way. It was shown that exponential type models present a realistic dark energy epoch that is compatible with local and observational tests [97]. The consideration of EC is crucial for exploring and establishing the existence of cosmic structures. Violations of these constraints are necessary for the formation of realistic WH configurations. In modified gravity, the violation of NEC guarantees the existence of a WH structure. For investigation of WH structures, we use $\mu = 1.8$, $\nu = 2$ and plot the graphs of ρ, $\rho + p_r$ and $\rho + p_t$. We plot the 3D graphs only for above chosen values. For other choices of μ and ν, We provide a 2D graphical analysis and present comprehensive details about these features in tabular form.

Figure 3 (left panel) presented the graphical behavior of the energy density ρ. The graph illustrates that the density is positive and exhibits a decreasing trend towards the boundary. Moreover, a region graph is also depicted (right panel) in which we can easily determine that $\rho > 0$ emphasized in yellow.

The graphical behavior of $\rho + p_r$ is presented in figure 4. In this context, we observe that the graph shows positive behavior in the range $2 \leqslant r/r_0 \leqslant 2.12$ and beyond this region violation of EC occurs. A region graph is also presented in which $\rho + p_r > 0$ highlighted in yellow and $\rho + p_r < 0$ is represented in red.

The graphical representation of $\rho + p_t$ is depicted in figure 5. We can notice that the graph shows positive behavior in the range of $2 \leqslant r/r_0 \leqslant 2.4$ and beyond this region violation of EC occurs. A region graph is also presented in which $\rho + p_t > 0$ shown in yellow.

Considering the exponential $f(\mathcal{R})$ gravity model, the summary of the analysis is as follows: (★) For $\mu = 1.8$, $\nu = 2$, we noticed that presence of EM at the throat can be prevented for the existence of traversable WH.

(★) From figure 4, $\rho + p_r$ is positive for the range $2 \leqslant r/r_0 \leqslant 2.12$, while $\rho + p_t$ and ρ are positive for $2 \leqslant r/r_0 \leqslant 4.3$ and $2 \leqslant r/r_0 \leqslant 3.3$ shown in figure 5 and 3, respectively . Hence NEC is respected for $2 \leqslant r/r_0 \leqslant 2.12$.

(★) In summary, the utilization of the exponential $f(\mathcal{R})$ gravity model, along with our selected shape function, $\mu = 1.8$, $\nu = 2$ are the acceptable parameters to obtain the traversable WH results in configurations featuring a small amount of EM content.

Furthermore, 2D graphical analysis of physical quantities ρ, $\rho + p_r$ and $\rho + p_t$ for different choices of parameters is also given below. It can be clearly visible from the figure 6 that

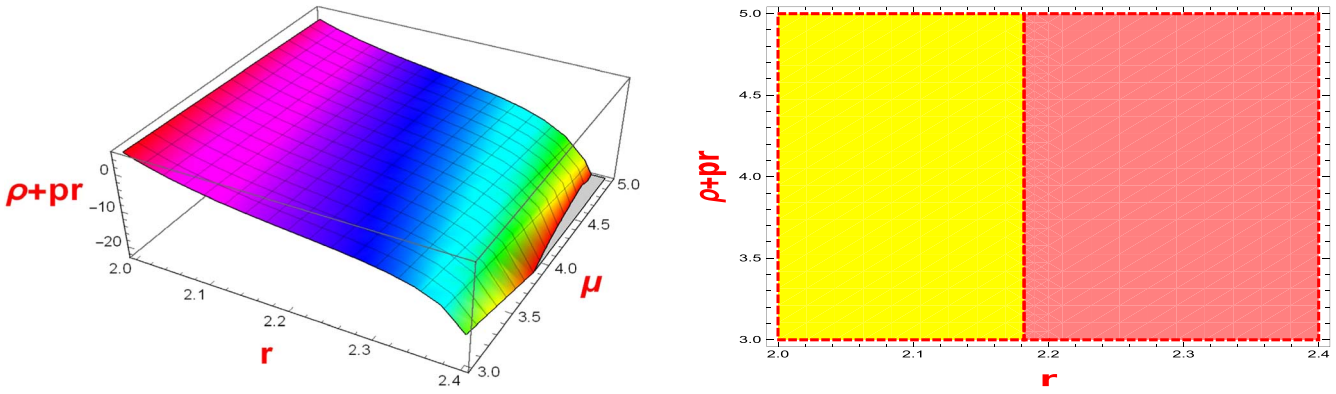

Figure 4. $\rho + p_{\rm r}$ graphs in 3D and region form.

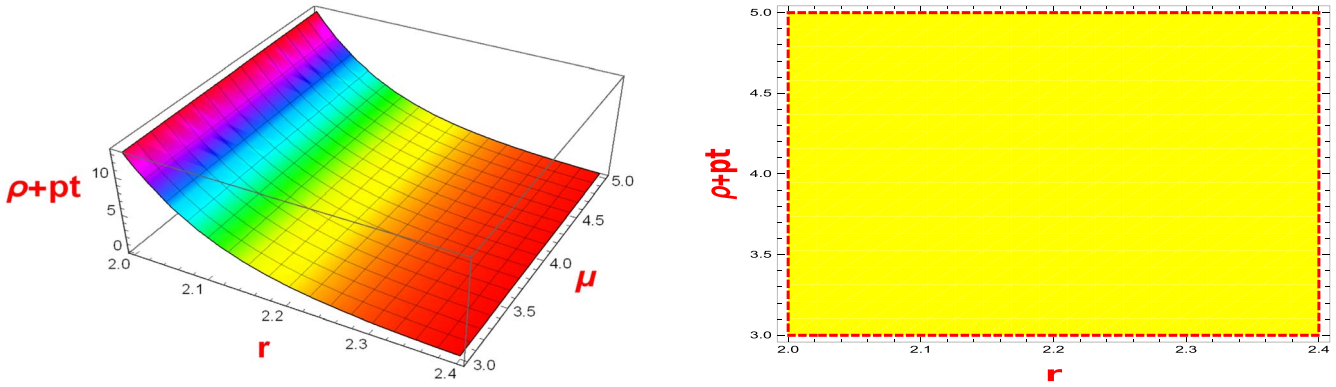

Figure 5. Represent the behavior of $\rho + p_{\rm t}$.

these features respect the EC near the throat. Comprehensive details for these features are also presented in table 1

3.2. Model 2: starobinsky gravity model

Secondly, we assume the $f_2(\mathcal{R})$ Starobinsky gravity model along with $f(\mathcal{G})$ power law model to investigate the solutions for WH in the corresponding gravity context. This most popular model is introduced by Starobinsky [98], which meets solar system and laboratory experiments and is compatible with cosmic conditions, given as

$$f_2(\mathcal{R}) = \mathcal{R} + \mu\,\nu[\left(1 + \frac{\mathcal{R}^2}{\nu^2}\right)^{-n} - 1], \tag{22}$$

where μ, ν and n are free parameters. In the literature, Model (21) contains properties of dark energy models and is consistent with cosmological and local gravity constraints [99]. It is used to investigate the effects of cosmic acceleration. For investigation, we choose $\mu = 2.5$, $\nu = 2$ and $n = 2$ to identify feasible traversable WH that exhibit a negligible amount of exotic matter at the throat. We plot the 3D graphs of ρ, $\rho + p_{\rm r}$ and $\rho + p_{\rm t}$ for above chosen values. For other choices of μ and ν, we provide a 2D graphical analysis and also present comprehensive details about these features in tabular form.

The pictorial representation of the density ρ is positive and exhibits a decreasing trend, as shown in the left panel of figure 7 and in the right panel, region graph is also presented in which we notice that $\rho > 0$ in complete region highlighted yellow.

The graphical behavior of $\rho + p_{\rm r}$ is presented in left panel of figure 8. One can easily seen that the graph shows positive behavior in the range $2 \leqslant r/r_0 \leqslant 2.4$ and beyond this region violation of EC occurs. A region graph is also shown in right panel, in which $\rho + p_{\rm r} > 0$ highlighted yellow.

The graphical representation of $\rho + p_{\rm t}$ is shown in the left panel of figure 9. The graph shows positive behavior in the range of $2 \leqslant r/r_0 \leqslant 3.7$ and beyond this range violation of EC occur. In right panel of figure 9, the region graph is also shown where $\rho + p_t > 0$ highlighted in yellow.

Considering the Starobinsky gravity model, the analysis is summarized as follows: (★) For $\mu = 2.5$, $\nu = 2$, we noticed that presence of EM at the throat can be prevented for the existence of traversable WH. (★) From figure 8, $\rho + p_{\rm r}$ is positive for the range $2 \leqslant r/r_0 \leqslant 2.4$, while $\rho + p_{\rm t}$ and ρ are positive for $2 \leqslant r/r_0 \leqslant 3.2$. Hence NEC is respected for $2 \leqslant r/r_0 \leqslant 2.4$. Hence, we can say that NEC is respected, demonstrating the absence of EM at the throat. Moreover, $\rho > 0$ prevents the amount of EM and generates a stable and traversable WH structure. (★) In conclusion, the utilization of this model together with our chosen shape function,

$\mu = 2.5$, $\nu = 2$ are the acceptable parameters to obtain the traversable WH configurations in absence of EM.

Moreover, 2D graphical analysis of physical quantities ρ, $\rho + p_{\rm r}$ and $\rho + p_{\rm t}$ for other choices of parameters for this

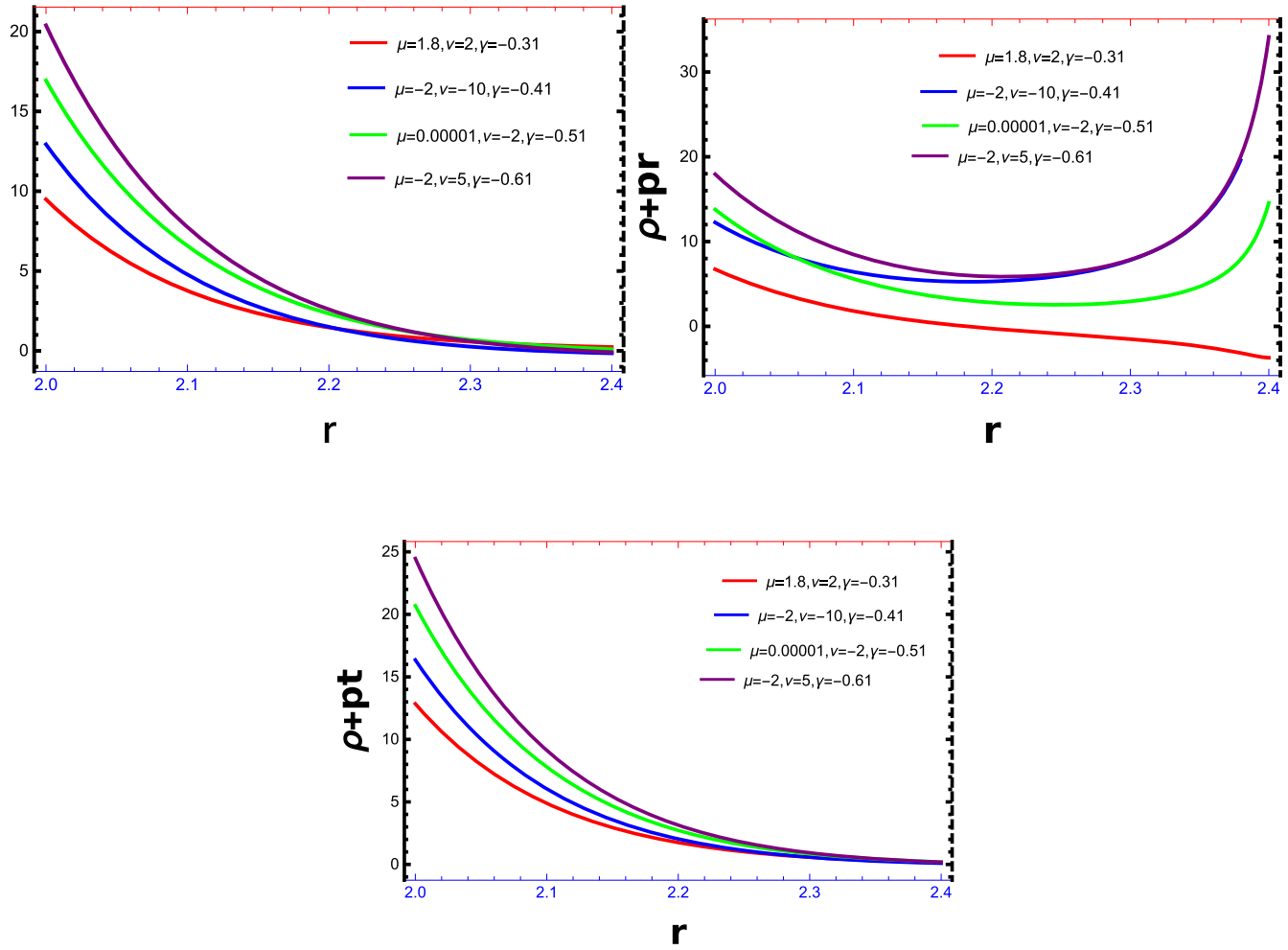

Figure 6. Shows the representation of ρ, $\rho + p_{\mathrm{r}}$ and $\rho + p_{\mathrm{t}}$ for Model 1.

Table 1. Summary of results for Model 1 under various parameters and energy conditions at $r_0 = 2$, $C = 1.9$.

Parameters conditions	Energy conditions	Energy conditions
$\mu, \nu > 0$	for $2 \leqslant r/r_0 \leqslant 3.3$ $\rho > 0$	for $\geqslant 3.4$ $\rho < 0$
$\mu, \nu < 0$	for $2 \leqslant r/r_0 \leqslant 3.0$ $\rho > 0$	for $\geqslant 3.1$ $\rho < 0$
$\mu > 0, \nu < 0$	for $2 \leqslant r/r_0 \leqslant 3.7$ $\rho > 0$	for $\geqslant 3.8$ $\rho < 0$
$\mu < 0, \nu > 0$	for $2 \leqslant r/r_0 \leqslant 3.3$ $\rho > 0$	for $\geqslant 3.4$ $\rho < 0$
	$\rho + p_{\mathrm{r}}$	
$\mu, \nu > 0$	for $2 \leqslant r/r_0 \leqslant 2.12$ $\rho + p_{\mathrm{r}} > 0$	for $\geqslant 2.13$ $\rho + p_{\mathrm{r}} < 0$
$\mu, \nu < 0$	for $2 \leqslant r/r_0 \leqslant 2.4$ $\rho + p_{\mathrm{r}} > 0$	for $\geqslant 2.5$ $\rho + p_{\mathrm{r}} < 0$
$\mu > 0, \nu < 0$	for $2 \leqslant r/r_0 \leqslant 2.4$ $\rho + p_{\mathrm{r}} > 0$	for $\geqslant 2.5$ $\rho + p_{\mathrm{r}} < 0$
$\mu < 0, \nu > 0$	for $2 \leqslant r/r_0 \leqslant 2.4$ $\rho + p_{\mathrm{r}} > 0$	for $\geqslant 2.5$ $\rho + p_{\mathrm{r}} < 0$
	$\rho + p_{t}$	
$\mu, \nu > 0$	for $2 \leqslant r/r_0 \leqslant 4.3$ $\rho + p_{\mathrm{t}} > 0$	for $\geqslant 4.4$ $\rho + p_{\mathrm{t}} < 0$
$\mu, \nu < 0$	for $2 \leqslant r/r_0 \leqslant 3.9$ $\rho + p_{\mathrm{t}} > 0$	for $\geqslant 4.0$ $\rho + p_{\mathrm{t}} < 0$
$\mu > 0, \nu < 0$	for $2 \leqslant r/r_0 \leqslant 4.1$ $\rho + p_{\mathrm{t}} > 0$	for $\geqslant 4.2$ $\rho + p_{\mathrm{t}} < 0$
$\mu < 0, \nu > 0$	for $2 \leqslant r/r_0 \leqslant 4.0$ $\rho + p_{\mathrm{t}} > 0$	for $\geqslant 4.1$ $\rho + p_{\mathrm{t}} < 0$

model is also presented below. It can be clearly visible from the 2D graphical analysis that these features respect the EC. Comprehensive details regarding these features are also furnished in table 2.

4. Comparison

Shamir and Fayyaz [100] constructed a WH shape function by applying the Karmarkar condition to a static traversable WH

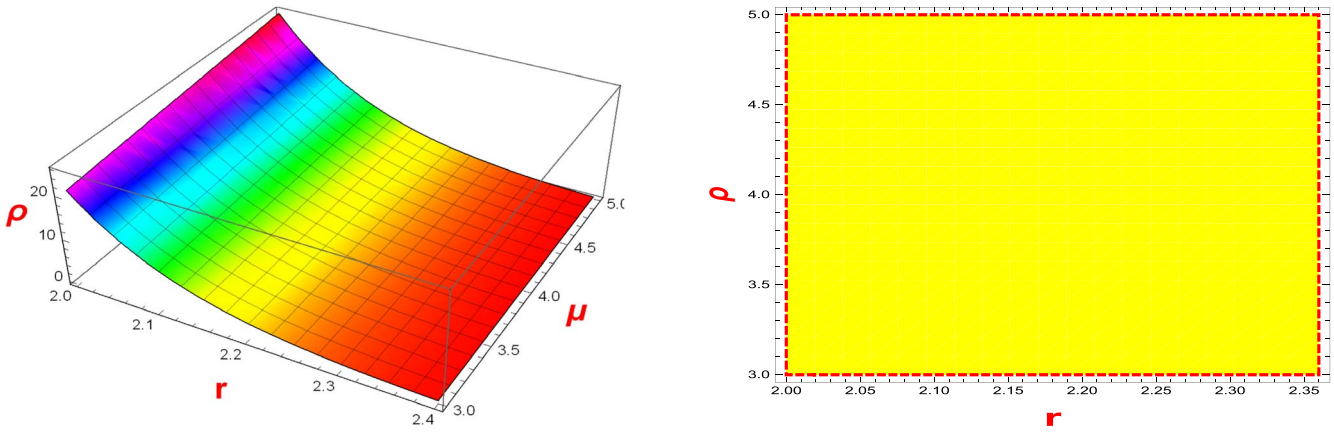

Figure 7. Shows the behavior ρ.

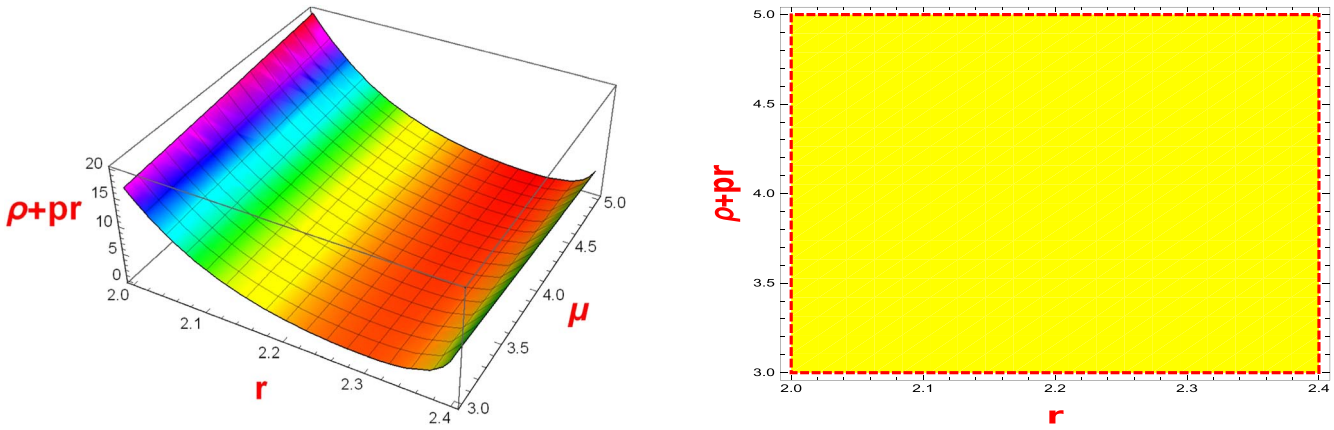

Figure 8. Shows the behavior $\rho + p_{\mathrm{r}}$.

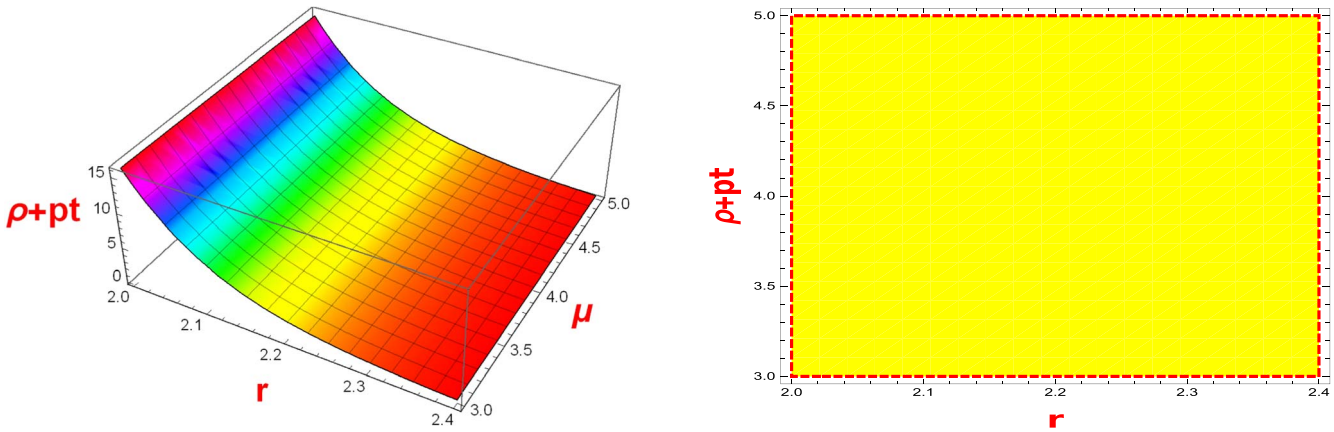

Figure 9. Shows the behavior $\rho + p_{\mathrm{t}}$.

geometry. They created a WH that connected two asymptotically flat regions of spacetime and satisfied the required conditions. A key aspect of our study is the examination and comparison of evolving WH geometries near the throat of our chosen models, accomplished through the use of two- and three-dimensional graphical representations. We have discussed the WH configurations in detail in framework of modified $f(\mathcal{R}, \mathcal{G})$ gravity. Moreover, the authors [100] considered viable and realistic $f(\mathcal{R})$ gravity models to discuss the WH geometry, but we have considered the combination of $f(\mathcal{R}, \mathcal{G})$ gravity model i.e. $f(\mathcal{R}, \mathcal{G}) = f(\mathcal{R}) + f(\mathcal{G})$ to investigate the behavior of traversable WHs, which make our work more generalized and comprehensive than the previous investigation. Godani and Samanta [101] discussed WH solutions in $f(\mathcal{R})$ gravity, focusing on specific $f(\mathcal{R})$ models and shape functions. In contrast, our approach involves constructing the shape function using the Karmarkar condition and exploring WH solutions across viable models, which

Table 2. Summary of results for Model 2 under various parameters and energy conditions at r_0=2, $C = 1.9$.

Parameters conditions	Energy conditions	Energy conditions
	ρ	
$\mu < 0, \nu < 0, n > 0$	for $2 \leqslant r/r_0 \leqslant 3.2$ $\rho > 0$	for $\geqslant 3.3$ $\rho < 0$
$\mu > 0, \nu > 0, n > 0$	for $2 \leqslant r/r_0 \leqslant 3.3$ $\rho > 0$	for $\geqslant 3.4$ $\rho < 0$
$\mu > 0, \nu > 0, n < 0$	for $2 \leqslant r/r_0 \leqslant 3.7$ $\rho > 0$	for $\geqslant 3.8$ $\rho < 0$
$\mu < 0, \nu < 0, n < 0$	for $2 \leqslant r/r_0 \leqslant 3.7$ $\rho > 0$	for $\geqslant 3.8$ $\rho < 0$
	$\rho + p_r$	
$\mu < 0, \nu < 0, n > 0$	for $2 \leqslant r/r_0 \leqslant 2.4 \rho + p_r > 0$	for $\geqslant 2.5$ $\rho + p_r < 0$
$\mu > 0, \nu > 0, n > 0$	for $2 \leqslant r/r_0 \leqslant 2.4$ $\rho + p_r > 0$	for $\geqslant 2.5$ $\rho + p_r < 0$
$\mu > 0, \nu > 0, n < 0$	for $2 \leqslant r/r_0 \leqslant 2.4$ $\rho + p_r > 0$	for $\geqslant 2.5$ $\rho + p_r < 0$
$\mu < 0, \nu < 0, n < 0$	for $2 \leqslant r/r_0 \leqslant 2.4$ $\rho + p_r > 0$	for $\geqslant 2.5$ $\rho + p_r < 0$
	$\rho + p_t$	
$\mu < 0, \nu < 0, n > 0$	for $2 \leqslant r/r_0 \leqslant 3.7$ $\rho + p_t > 0$	for $\geqslant 3.8$ $\rho + p_t < 0$
$\mu > 0, \nu > 0, n > 0$	for $2 \leqslant r/r_0 \leqslant 3.9 \rho + p_t > 0$	for $\geqslant 4.0$ $\rho + p_t < 0$
$\mu > 0, \nu > 0, n < 0$	for $2 \leqslant r/r_0 \leqslant 4.1$ $\rho + p_t > 0$	for $\geqslant 4.2$ $\rho + p_t < 0$
$\mu < 0, \nu < 0, n < 0$	for $2 \leqslant r/r_0 \leqslant 4.1$ $\rho + p_t > 0$	for $\geqslant 4.2$ $\rho + p_t < 0$

distinguishes our work. Sharif and Fatima [102] analyzed traversable WH solutions in $f(\mathcal{R}, \mathcal{T})$ gravity, considering specific $f(\mathcal{R}, \mathcal{T})$ models and fixed parameters for simplicity. In our current work, we investigate traversable WH solutions in $f(\mathcal{R}, \mathcal{G})$ gravity models where we explore the interaction between the Ricci scalar $\mathcal{G}$ and Gauss–Bonnet term $\mathcal{G}$, presenting a novel perspective compared to previous research. Banerjee *et al* [103] presented static and spherically symmetric WH solutions using specific choices for the $f(\mathcal{Q})$ form and constant redshift, whereas our analysis involves constructing WH geometries and investigating energy conditions across various scenarios. Mishra *et al* [104] discussed traversable WH geometry using three shape functions and constant redshift, while our analysis differs as we adopt a more general redshift function dependent on the radial coordinate r, which make our work different from the previous one.

5. Concluding remarks

Modified theories of gravity is nowadays an extremely important tool to address some persistent observational issues, such as the dark sector of the Universe. They are also applicable to stellar astrophysics, potentially yielding insights beyond those provided by GR. In this article, we explore a novel $f(\mathcal{R}, \mathcal{G})$ gravity model within the context of WH physics and geometry. The modified $f(\mathcal{R}, \mathcal{G})$ gravity is a prominent alternative theory where the Ricci scalar $\mathcal{R}$ in the Einstein–Hilbert gravitational Lagrangian is replaced by a general function of $\mathcal{R}$ and $\mathcal{G}$, with $\mathcal{G}$ representing the Gauss–Bonnet term. We derive the field equations, solving them to obtain the WH metric and energy-momentum tensor. The significance of applying alternative gravity theories to WHs lies in the possibility of finding WH solutions that satisfy ECs, deviating from the outcomes predicted by GR. The main motivation for working with WHs within alternative gravity models is the possibility of obtaining WH solutions satisfying the ECs, departing from the GR case [4]. In fact, such a feature has already been attained through other MTG [105–107].

Achieving spherical symmetry is a fundamental prerequisite for modeling static traversable WH. Various approaches have been proposed in the literature to acquire viable WH solutions. One approach involves determining the WSF by assuming properties of the matter components, while another approach explores how well the EC are satisfied with the consideration of the shape function. In this study, we formulate a WSF using the Karmarkar criterion. The aim is to investigate the evolving embedded WH solutions within the framework of $f(\mathcal{R}, \mathcal{G})$ gravity, considering two viable models. The WH solution must violate the EC in the context of GR. In contrast, it is possible to discover a WH configurations in modified theories that respects NEC at the throat. A captivating element of this study involves conducting a comparative examination of the evolving geometries of WH near the throat in the models under consideration. This analysis is facilitated through the use of two and three-dimensional graphical representations. We observe that our shape function acquired through the Karmarkar technique yields validated WH configurations with even less EM correlating to the proper choice of $f(\mathcal{R}, \mathcal{G})$ gravity models and acceptable free parameter values. We have only plotted the graphs for those specific parametric values when these features show positive behavior i.e. $\rho > 0$, $\rho + p_r > 0$ and $\rho + p_t > 0$, while for the other choice of parameters we have shown the analysis in tables 1 and 2 where $\rho < 0$, $\rho + p_r < 0$ and $\rho + p_t < 0$. To verify this, Moreover, we look at precise answers for static spherically symmetric traversable WH geometry within the framework of $f(\mathcal{R}, \mathcal{G})$ gravity.

- We start by considering the exponential gravity model i.e. $f_1(\mathcal{R}) = \mathcal{R} + \mu\ \nu[e^{\frac{-\mathcal{R}}{\nu}} - 1]$, along with the power law model given as $f(\mathcal{G}) = \gamma\mathcal{G}^2$, to show the feasibility of a static spherically symmetric traversable *WH*, where μ, ν and γ are free parameters. We also discussed the EC for these parameters $\mu = 1.8$, $\nu = 2$ and $\gamma = -0.31$. The graphical analysis of *EC* in 2D and 3D is shown in

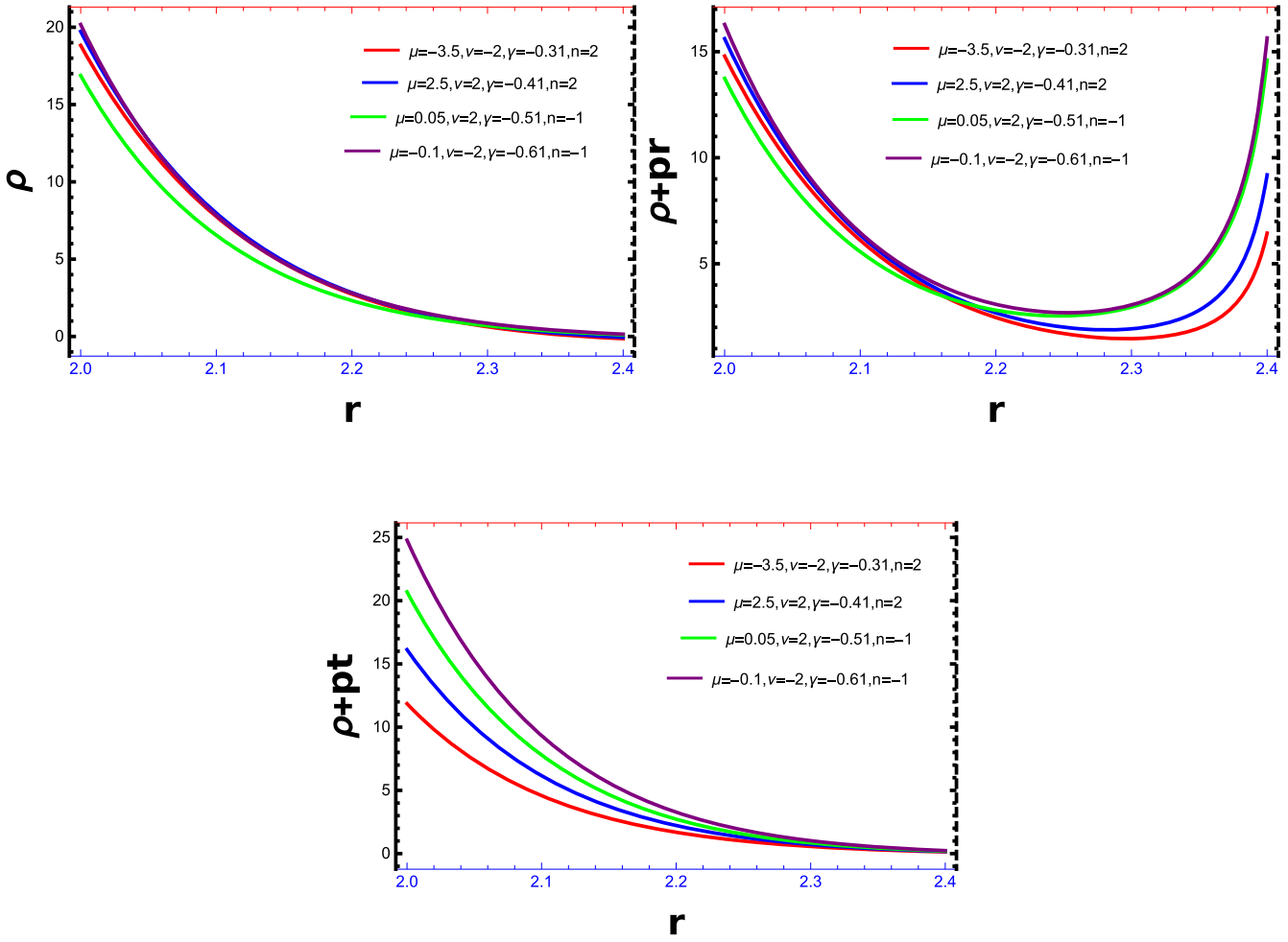

Figure 10. Shows the behavior ρ, $\rho + p_{\mathrm{r}}$ and $\rho + p_{\mathrm{t}}$ for Model 2.

Table 3. Comparison of models $r_0 = 2$, $C = 1.9$.

Physical quantities	Exponential and power law model	Starobinsky and power law model
ρ	>0 for $2 \leqslant r/r_0 \leqslant 3.3$ <0 for $\geqslant 3.4$	>0 for $2 \leqslant r/r_0 \leqslant 3.2$ <0 for $\geqslant 3.3$
$\rho + p_{\mathrm{r}}$	>0 for $2 \leqslant r/r_0 \leqslant 2.2$ <0 for $\geqslant 2.3$	>0 for $2 \leqslant r/r_0 \leqslant 2.4$ <0 for $\geqslant 2.5$
$\rho + p_{\mathrm{t}}$	>0 for $2 \leqslant r/r_0 \leqslant 4.0$ <0 for $\geqslant 4.1$	>0 for $2 \leqslant r/r_0 \leqslant 3.7$ <0 for $\geqslant 3.8$

figures 3–6. One can easily observed that these EC are respected at the throat for some certain region. Further we have also concluded that $\mu > 0$, $\nu > 0$ and $\gamma < 0$ is the appropriate combination to get WH solutions with the presence of negligible amount of EM. Moreover, near the throat the NEC is respected, the detailed analysis is presented in table 1.

- Secondly, we consider Starobinsky $f(\mathcal{R})$ gravity model i.e. $f_2(\mathcal{R}) = \mathcal{R} + \mu\ \nu\left[\left(1 + \frac{\mathcal{R}^2}{\nu^2}\right)^{-n} - 1\right]$, along with same power law model given as $f(\mathcal{G}) = \gamma\mathcal{G}^2$, to discuss the possibility of static spherically symmetric traversable WH, where μ, ν, n and γ are free parameters. The EC are discussed for chosen parametric values i.e. $\mu = 2.5$, $\nu = 2$, $n = 2$ and $\gamma = -0.41$. The 2D and 3D graphical analysis of these EC is presented in figures 7–10. One can easily observed that these EC are respected near the throat as well as for larger region. The detailed analysis about these conditions is given in table 2.
- For the evolving embedded traversable WH solutions, we have also presented the comparative analysis of both models in tabular form given in table 3. It can be easily seen from the table 3 that Starobinsky model provides traversable WH solutions with less amount of EM in the context of $f(\mathcal{R}, \mathcal{G})$ gravity. In framework of $f(\mathcal{R}, \mathcal{G})$ gravity our results respect ECs not only at throat also for some larger values of radial coordinate r.

Fayyaz and Shamir [108] successfully identified the feasibility and stability of constructing traversable WH in the presence of EM using the GR paradigm. Additionally, the same authors [100] concluded that, for a specific shape function, a WH solution exists in the $f(\mathcal{R})$ theory with a constrained quantity of EM.

It is important to highlight that our results confirm the NEC and even the WEC within the framework of $f(\mathcal{R}, \mathcal{G})$ gravity, more significant values of the radial coordinate r, rather than exactly at the throat. Thus, we come to the conclusion that our proposed models and the specified WSF demonstrate the formation of traversable WH configurations within the framework of $f(\mathcal{R}, \mathcal{G})$ gravity, featuring a very negligible amount of EM.

Indeed, our results demonstrate that WH solutions satisfying the ECs can be achieved within the frame of modified $f(\mathcal{R}, \mathcal{G})$ gravity. There remains considerable work to be done with these models by incorporating charge, particularly in its applications to cosmology, galactic dynamics, and stellar astrophysics. Readers are encouraged to further explore these possibilities. Nonetheless, the present results provide a promising indication of the theory's potential. Future research should also aim to explore WH geometries in a more generalized framework. This could provide valuable insights into constructing traversable WHs without relying on EM, potentially broadening the scope of feasible WH models.

Acknowledgments

First author TN would like to acknowledge National University of Computer and Emerging Sciences (NUCES) for funding support through research reward programme. Second Author AM acknowledges the Grant No. YS304023912 to support his Postdoctoral Fellowship at Zhejiang Normal University, China.

References

[1] Einstein A and Rosen N 1935 The particle problem in the general theory of relativity *Phys. Rev.* **48** 73
[2] Flamm L 1916 Comments on Einstein's theory of gravity *Physikalische Zeitschrift* **17** 448
[3] Kar S 1994 Evolving wormholes and the weak energy condition *Phys. Rev.* D **49** 862
[4] Morris M S and Thorne K S 1988 Wormholes in spacetime and their use for interstellar travel: A tool for teaching general relativity *Am. J. Phys.* **56** 395–412
[5] Capozziello S and De Laurentis M 2011 Extended theories of gravity *Phys. Rep.* **509** 167–321
[6] Nojiri S and Odintsov SD 2011 Unified cosmic history in modified gravity: from $F(R)$ theory to Lorentz non-invariant models *Phys. Rep.* **505** 59–144
[7] Clifton T *et al* 2012 Modified gravity and cosmology *Phys. Rep.* **513** 1–189
[8] Berti E *et al* 2015 Testing general relativity with present and future astrophysical observations *Class. Quantum. Grav.* **32** 243001
[9] Nojiri S S D O and Oikonomou V K 2017 Modified gravity theories on a nutshell: inflation, bounce and late-time evolution *Phys. Rep.* **692** 1–104
[10] Buchdahl H A 1970 Non-linear Lagrangians and cosmological theory *Mon. Not. R. Astron. Soc.* **150** 1–8
[11] Starobinsky A A 1980 A new type of isotropic cosmological models without singularity *Phys. Lett.* B **91** 99–102
[12] Nojiri S and Odintsov S D 2003 Modified gravity with negative and positive powers of curvature: unification of inflation and cosmic acceleration *Phys. Rev.* D **68** 123512
[13] Astashenok A V and Odintsov S D 2016 From neutron stars to quark stars in mimetic gravity *Phys. Rev.* D **94** 063008
[14] Astashenok A V, Capozziello S and Odintsov S D 2015 Nonperturbative models of quark stars in $f(R)$ gravity *Phys. Lett.* B **742** 160–6
[15] Nashed G G L 2021 Anisotropic compact stars in the mimetic gravitational theory *Astrophys. J.* **919** 113
[16] Rashid A, Malik A and Shamir M F 2023 A comprehensive study of Bardeen stars with conformal motion in $f(G)$ gravity *Eur. Phys. J.* C **83** 997
[17] Malik A *et al* 2024 Study of traversable wormhole solutions via Karmarkar condition in $f(R, \phi, X)$ theory of gravity *The European Physical Journal Plus* **139** 101
[18] Asghar Z *et al* 2023 Comprehensive analysis of relativistic embedded class-I exponential compact spheres in $f(R, \phi)$ gravity via Karmarkar condition *Commun. Theor. Phys.* **75** 105401
[19] Naz T *et al* 2023 Evolving embedded traversable wormholes in $f(R, G)$ gravity: a comparative study *Phys. Dark. Uni.* **42** 101301
[20] Chalavadi C C *et al* 2024 Exploration of GUP-corrected Casimir wormholes in extended teleparallel gravity with matter coupling *Nucl. Phys.* B 116644
[21] Malik A *et al* 2024 Charged wormhole solutions utilizing Karmarkar condition in Ricci inverse gravity *Eur. Phys. J. Plus.* **139** 535
[22] Fayyaz I, Naz T and Malik A 2024 Fate of charged wormhole structures utilizing Karmarkar approach *New Astron.* **112** 102255
[23] Malik A *et al* 2023 Investigation of traversable wormhole solutions in modified $f(R)$ gravity with scalar potential *Eur. Phys. J.* C **83** 1–12
[24] Riess A G *et al* 2001 The farthest known supernova: support for an accelerating universe and a glimpse of the epoch of deceleration *Astrophys. J.* **560** 49
[25] Perlmutter S *et al* 1999 Constraining dark energy with type Ia supernovae and large-scale structure *Phys. Rev. Lett.* **83** 670
[26] Hinshaw G *et al* 2003 First-year Wilkinson microwave anisotropy probe observations: data processing methods and systematic error limits *Astrophys. J. Suppl. Ser.* **148** 63
[27] Nandi K K, Islam A and Evans J 1997 Brans wormholes *Phys. Rev.* D **55** 2497
[28] Lobo FSN and Oliveira MA 2010 General class of vacuum Brans-Dicke wormholes *Phys. Rev.* D **81** 067501
[29] Richarte M G and Simeone C 2009 Wormholes in Einstein-Born-Infeld theory *Phys. Rev.* D **80** 104033
[30] Mehdizadeh M R, Zangeneh M K and Lobo FSN 2015 Einstein-Gauss-Bonnet traversable wormholes satisfying the weak energy condition *Phys. Rev.* D **91** 084004
[31] Dzhunushaliev V and Singleton D 1999 Wormholes and flux tubes in 5D Kaluza-Klein theory *Phys. Rev.* D **59** 064018
[32] Shaikh R and Kar S 2016 Wormholes, the weak energy condition, and scalar-tensor gravity *Phys. Rev.* D **94** 024011
[33] Mehdizadeh MR and Ziaie A H 2017 Einstein-Cartan wormhole solutions *Phys. Rev.* D **95** 064049
[34] Sharif M and Zahra Z 2013 Static wormhole solutions in $f(R)$ gravity *Astrophys. Space Sci.* **348** 275–82
[35] Mishra A K *et al* 2020 Traversable wormholes in $f(R, T)$ gravity *Astrophys. Space Sci.* **365** 34
[36] Shamir M F and Zia S 2018 Existence of static wormhole solutions in $f(R, G)$ gravity *Astrophys. Space Sci.* **363** 247
[37] Mazharimousavi S H, Halilsoy M and Amirabi Z 2010 Higher-dimensional thin-shell wormholes in Einstein-Yang-Mills-Gauss-Bonnet gravity *Classical Quantum Gravity* **28** 025004
[38] Bhattacharya S and Chakraborty S 2017 $f(R)$ gravity solutions for evolving wormholes *Eur. Phys. J.* C **77** 1–9
[39] Sahoo P K *et al* 2018 Phantom fluid supporting traversable wormholes in alternative gravity with extra material terms *Int. J. Mod. Phys.* D **27** 1950004

[40] Sahoo P K, Moraes P H R S and Sahoo P 2018 Wormholes in R 2-gravity within the $f(R, T)$ formalism *Eur. Phys. J.* C **78** 1–7

[41] Liu W-M, Wu B and Niu Q 2000 Nonlinear effects in interference of Bose-Einstein condensates *Phys. Rev. Lett.* **84** 2294

[42] Liang Z X, Zhang Z D and Liu W M 2005 Dynamics of a bright soliton in Bose-Einstein condensates with time-dependent atomic scattering length in an expulsive parabolic potential *Phys. Rev. Lett.* **94** 050402

[43] Ji A-C *et al* 2008 Dynamical creation of fractionalized vortices and vortex lattices *Phys. Rev. Lett.* **101** 010402

[44] Malik A *et al* 2022 Traversable wormhole solutions in the $f(R)$ theories of gravity under the Karmarkar condition *Chin. Phys.* C **46** 095104

[45] Malik A and Nafees A 2021 Existence of static wormhole solutions using $f(R, \phi, X)$ theory of gravity *New Astron.* **89** 101632

[46] Shamir M F, Malik A and Mustafa G 2021 Wormhole solutions in modified $f(R, \phi, X)$ gravity *Int. J. Mod. Phys.* A **36** 2150021

[47] Nojiri S *et al* 2024 Wormholes inside stars and black holes *Phys. Rev.* D **109** 104007

[48] Bahamonde S *et al* 2016 Scalar-tensor teleparallel wormholes by Noether symmetries *Phys. Rev.* D **94** 084042

[49] Samanta G C and Godani N 2019 Wormhole modeling supported by non-exotic matter *Mod. Phys. Lett.* A **34** 1950224

[50] Cataldo M, Liempi L and Rodrguez P 2017 Traversable Schwarzschild-like wormholes *Eur. Phys. J.* C **77** 748

[51] Jahromi A S and Moradpour H 2018 Static traversable wormholes in Lyra manifold *Int. J. Mod. Phys.* D **27** 1850024

[52] Samanta G C, Godani N and Bamba K 2020 Traversable wormholes with exponential shape function in modified gravity and general relativity: A comparative study *Int. J. Mod. Phys.* D **29** 2050068

[53] Nash J 1956 The imbedding problem for Riemannian manifolds *Annals of Mathematics* **63** 20–63

[54] Kohler M and Chao K L 1965 Zentralsymmetrische statische Schwerefelder mit R?umen der Klasse 1 *Zeitschrift für Naturforschung* A **20** 1537–43

[55] Maurya S K *et al* 2016 A new exact anisotropic solution of embedding class one *Eur. Phys. J.* A **52** 191

[56] Bhar P *et al* 2016 Modelling of anisotropic compact stars of embedding class one *Eur. Phys. J.* A **52** 312

[57] Deb D *et al* 2019 Exploring physical features of anisotropic strange stars beyond standard maximum mass limit in gravity *Mon. Not. R. Astron. Soc.* **485** 5652–65

[58] Peter KF 2018 Two diverse models of embedding class one *Ann. Phys.* **392** 63–70

[59] Kuhfittig PKF 2019 Spherically symmetric wormholes of embedding class one *Pramana* **92** 75

[60] Maurya S K and Maharaj S D 2018 New anisotropic fluid spheres from embedding *Eur. Phys. J.* A **54** 1–11

[61] Maurya S K *et al* 2017 Compact stars with specific mass function *Ann. Phys.* **385** 532–45

[62] Gupta Y K and Gupta R S 1986 Nonstatic analogues of Kohler-Chao solution of imbedding class one *Gen. Relativ. Gravitation* **18** 641–8

[63] Gupta Y K and Sharma J R 1996 Non-static non-conformally flat fluid plates of embedding class one *Gen. Relativ. Gravitation* **28** 1447–53

[64] Karmarkar K R 1948 *Gravitational Metrics of Spherical Symmetry and Class One. Proceedings of the Indian Academy of Sciences-Section A* Vol. 27 (Springer) (https://doi.org/10.1007/BF03173443)

[65] Maurya S K *et al* 2016 A new model for spherically symmetric anisotropic compact star *Eur. Phys. J.* C **76** 1–9

[66] Waheed S *et al* 2020 Physically acceptable embedded class-I compact stars in modified gravity with Karmarkar condition *Symmetry* **12** 962

[67] Abbas G *et al* 2019 Quintessence compact stars satisfying Karmarkar condition *Can. J. Phys.* **97** 374–81

[68] Maurya S K *et al* 2016 Generalised model for anisotropic compact stars *Eur. Phys. J.* C **76** 1–12

[69] Bhar P 2017 Modelling a new class of anisotropic compact stars satisfying the Karmakar's condition *Eur. Phys. J. Plus.* **132** 1–12

[70] Sharif M and Saba S 2020 Embedding class-1 anisotropic solution in $f(G)$ gravity *Chin. J. Phys.* **64** 374–89

[71] Upreti J *et al* 2020 Relativistic parametric embedding class I solutions of cold stars in Karmarkar space-time continuum *New Astron.* **80** 101403

[72] Ruderman M 1972 Pulsars: structure and dynamics *Annu. Rev. Astron. Astrophys.* **10** 427

[73] Canuto V and Chitre S M 1973 Solidification of neutron matter *Phys. Rev. Lett.* **30** 999

[74] Canuto V and Chitre S M 1974 Crystallization of dense neutron matter *Phys. Rev.* D **9** 1587

[75] Canuto V 1974 Equation of state at ultrahigh densities. I *Annu. Rev. Astron. Astrophys.* **12** 167–214 (A75-13476 03-90) Palo Alto, Calif., Annual Reviews, Inc., 12

[76] Vittorio Canuto 1975 Equation of state at ultrahigh densities. II *Annu. Rev. Astron. Astrophys.* **13** 335–80 (A76-10076 01-88) Palo Alto, Calif., Annual Reviews, Inc., 13

[77] Canuto V 1977 Neutron stars: general review *Ann. N.Y. Acad. Sci.* **302** 514–27

[78] Bowers R L and Liang E P T 1974 Anisotropic spheres in general relativity *Astrophys. J.* **188** 657

[79] Sawyer R F 1972 Condensed p-phase in neutron-star matter *Phys. Rev. Lett.* **29** 382

[80] Angela P 1995 Three new magnetic white dwarf stars *Astrophys. J.* **451** L67

[81] Reimers D *et al* 1996 Discovery of four white dwarfs with strong magnetic fields by the Hamburg/ESO Survey arXiv: astro-ph/9604104

[82] Martinez A P, González Felipe R and Manreza Paret D 2010 Mass-radius relation for strange quarks Stars *Int. J. Mod. Phys.* D **19** 1511–9

[83] Abbas G *et al* 2018 Compact stars of emending class one in f (T) gravity *Iran. J. Sci. Technol. Trans. Sc.* **42** 1659–68

[84] Pratibha F and Pant N 2017 Physical plausibility of cold star models satisfying Karmarkar conditions *Eur. Phys. J.* A **53** 1–9

[85] Piyali B, Singh K N and Manna T 2017 A new class of relativistic model of compact stars of embedding class I *Int. J. Mod. Phys.* D **26** 1750090

[86] Satyanarayana G, Bisht RK and Pant N 2018 Stellar modelling of PSR J1614-2230 using the Karmarkar condition *Eur. Phys. J.* A **54** 207

[87] Maurya S K *et al* 2016 Generalised model for anisotropic compact stars *Eur. Phys. J.* C **76** 1–12

[88] Salako I G *et al* 2020 Study on anisotropic strange stars in $f(T, T)$ gravity *Universe* **6** 167

[89] Tayyaba N, Usman A and Farasat Shamir M 2021 Embedded class-I solution of compact stars in $f(R)$ gravity with Karmarkar condition *Ann. Phys.* **429** 168491

[90] Riaz A and Abbas G 2020 Non-adiabatic gravitational collapse in $f(R, T)$ gravity with Karmarkar condition for anisotropic fluid *Mod. Phys. Lett.* A **35** 2050103

[91] Kuhfittig P K F 2019 Spherically symmetric wormholes of embedding class one *Pramana* **92** 75

[92] Krori K D and Barua J 1975 A singularity-free solution for a charged fluid sphere in general relativity *J. Phys. A: Math. Gen.* **8** 508

[93] Atazadeh K and Darabi F 2014 Energy conditions in $f(R, G)$ gravity *Gen. Relativ. Gravitation* **46** 1–14

[94] Misner C W and Sharp DH 1964 Relativistic equations for adiabatic, spherically symmetric gravitational collapse *Phys. Rev.* **136** B571
[95] Gutfreund H and Jürgen R 2017 *The Formative Years of Relativity: The History and Meaning of Einstein's Princeton Lectures* (Princeton University Press)
[96] Cognola G *et al* 2008 Class of viable modified $f(R)$ gravities describing inflation and the onset of accelerated expansion *Phys. Rev.* D **77** 046009
[97] Linder E V 2009 Exponential gravity *Phys. Rev.* D **80** 123528
[98] Starobinsky A A 2007 Disappearing cosmological constant in $f(R)$ gravity *JETP Lett.* **86** 157–63
[99] Tsujikawa S 2010 *Modified Gravity Models of Dark Energy. Lectures on Cosmology: Accelerated Expansion of the Universe* (Springer) 99–145
[100] Shamir M F and Fayyaz I 2020 Traversable wormhole solutions in $f(R)$ gravity via Karmarkar condition *Eur. Phys. J.* C **80** 1–9
[101] Godani N and Samanta G C 2020 Traversable wormholes in $f(R)$ gravity with constant and variable redshift functions *New Astron.* **80** 101399
[102] Sharif M and Fatima A 2023 Traversable wormhole solutions admitting Karmarkar condition in $f(R, T)$ theory *Eur. Phys. J. Plus* **138** 196
[103] Banerjee A *et al* 2021 Wormhole geometries in $f(Q)$ gravity and the energy conditions *Eur. Phys. J.* C **81** 1–7
[104] Mishra B *et al* 2022 Traversable wormhole models in $f(R)$ gravity *Int. J. Mod. Phys.* A **37** 2250010
[105] Mehdizadeh M R and Ziaie A H 2017 Dynamic wormhole solutions in Einstein-Cartan gravity *Phys. Rev.* D **96** 124017
[106] Mehdizadeh M R and Ziaie A H 2017 Einstein-Cartan wormhole solutions *Phys. Rev.* D **95** 06404
[107] Mehdizadeh M R, Zangeneh M K and Lobo F S N 2015 Higher-dimensional thin-shell wormholes in third-order Lovelock gravity *Phys. Rev.* D **92** 044022
[108] Fayyaz I and Farasat Shamir M 2020 Morris-Thorne wormhole with Karmarkar condition *Chin. J. Phys.* **66** 553–9